BIOMACROMOLECULES

ARTICLE

pubs.acs.org/Biomac

Neutron Reflectometry and QCM-D Study of the Interaction of Cellulases with Films of Amorphous Cellulose

Gang Cheng,[†,‡] Zelin Liu,[§,○] Jaclyn K. Murton,[‡] Michael Jablin,[∥] Manish Dubey,[∥] Jaroslaw Majewski,[∥] Candice Halbert,[⊥] James Browning,[⊥] John Ankner,[⊥] Bulent Akgun,[#,▽] Chao Wang,[§] Alan R. Esker,[§] Kenneth L. Sale,[†,‡] Blake A. Simmons,[†,‡] and Michael S. Kent[*,†,‡]

[†]Joint BioEnergy Institute, Emeryville, California

[‡]Sandia National Laboratories, Livermore, California and Albuquerque, New Mexico

[§]Department of Chemistry, Virginia Polytechnic Institute and State University, Blacksburg, Virginia

[∥]Lujan Neutron Science Center, Los Alamos National Laboratories, Los Alamos, New Mexico

[⊥]Spallation Neutron Source, Oak Ridge National Laboratory, Oak Ridge, Tennessee

[#]National Institute of Standards and Technology, Gaithersburg, Maryland

[▽]Department of Materials Science and Engineering, University of Maryland, College Park, Maryland

Supporting Information

ABSTRACT: Improving the efficiency of enzymatic hydrolysis of cellulose is one of the key technological hurdles to reduce the cost of producing ethanol and other transportation fuels from lignocellulosic material. A better understanding of how soluble enzymes interact with insoluble cellulose will aid in the design of more efficient enzyme systems. We report a study involving neutron reflectometry (NR) and quartz crystal microbalance with dissipation monitoring (QCM-D) of the interaction of a fungal enzyme extract (*T. viride*) and an endoglucanse from *A. niger* with amorphous cellulose films. The use of amorphous cellulose is motivated by that the fact that several biomass pretreatments currently under investigation disrupt the native crystalline structure of cellulose and increase the amorphous content. NR reveals the profile of water through the film at nanometer resolution and is highly sensitive to interfacial roughness, whereas QCM-D provides changes in mass and film stiffness. NR can be performed using either H_2O- or D_2O-based aqueous reservoirs. NR measurement of swelling of a cellulose film in D_2O and in H_2O revealed that D/H exchange on the cellulose chains must be taken into account when a D_2O-based reservoir is used. The results also show that cellulose films swell slightly more in D_2O than in H_2O. Regarding enzymatic digestion, at 20 °C in H_2O buffer the *T. viride* cocktail rapidly digested the entire film, initially roughening the surface, followed by penetration and activity throughout the bulk of the film. In contrast, over the same time period, the endoglucanase was active mainly at the surface of the film and did not increase the surface roughness.

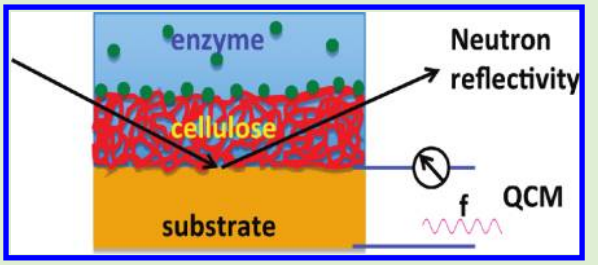

INTRODUCTION

Growing interest in alternative and renewable energy sources has brought increasing attention to the utilization of lignocellulosic materials to produce fuels and useful chemicals.[1] Conversion of lignocellulosic materials typically involves three steps: pretreatment of the biomass, enzymatic hydrolysis of cellulose and hemicellulose to fermentable sugars, and fermentation of the sugars to liquid fuels or other products.[2] The efficiency of hydrolysis, which is one of the primary obstacles to commercializing the process, can in principle be enhanced by mitigating the inherent recalcitrance of biomass through pretreatment or genetic modification of plant cell walls and by designing highly efficient enzymes.[3−5] The various pretreatments that are currently being explored have different effects on the physical nature of cellulose, and enzyme cocktails must be optimized for each particular pretreatment. Following the demonstration that ionic liquids (ILs) are solvents for cellulose and for lignocellulosic biomass under relatively mild processing conditions, they have been increasingly examined for biomass pretreatment.[6,7] Enzymatic hydrolysis of cellulose is greatly enhanced after IL pretreatment of biomass as the pretreatment destroys the native cellulose crystal structure and the lignin−hemicellulose network. Depending upon the conditions, the pretreated cellulose may be largely amorphous or may contain substantial cellulose II structure.[6−9] Other pretreatments such as ammonia fiber expansion (AFEX), ammonia recycle percolation (ARP), and phosphoric acid also disrupt the native cellulose structure and substantially increase the amorphous content.[10−12] This motivates the

Received: March 4, 2011
Revised: May 7, 2011
Published: May 09, 2011

present study of cellulases interacting with amorphous cellulose films.

Cellulases have traditionally been divided into endo- and exoglucanases. Endoglucanases hydrolyze the β-1,4-glycosidc bonds randomly along the chain, whereas exoglucanases (or cellobiohydrolases) hydrolyze from the chain ends in a processive manner and release cellobiose.[5] In addition, β-glucosidases convert cellobiose units to glucose. Each enzyme type plays a distinct role in the process, and the various enzymes must work synergistically for highly efficient hydrolysis of crystalline cellulose. Synergism occurs when the activity exhibited by mixtures of components is greater than the sum of the activity of the components evaluated separately.[13−15] Whereas enzyme synergy has long been known to be important for efficient digestion of crystalline cellulose, recent observations have demonstrated that enzyme synergy is important for digestion of amorphous cellulose as well.[13] There is therefore a need for methods that can resolve the behavior of individual enzymes on amorphous cellulose films.

Cellulose thin films have been used as a well-controlled model substrate to investigate the physical actions of cellulases by ellipsometry and quartz crystal microbalance with dissipation monitoring (QCM-D).[5,13,16−18] With QCM-D, changes in frequency and energy dissipation of an oscillating crystal coated with a cellulose film are monitored that are indicative of changes in mass and film stiffness, respectively, with enzymatic activity.[5,13] Here we introduce neutron reflectivity (NR) as another nonintrusive technique, highly complementary to QCM-D, to probe the structural changes in cellulose films resulting from the actions of cellulases. NR reveals the profile of neutron scattering length density (SLD) perpendicular to the film at nanometer resolution, which is determined by the density and atomic composition.[19] In this work, NR was used to determine the volume fraction profile of water through cellulose thin films. Such data reveal whether an enzyme acts on the surface or throughout the bulk of the film and whether its activity results in removal of mass, increased water content, or changes in surface roughness. Therefore, the combination of QCM-D and NR is highly complementary and can provide a wealth of detailed information about the interactions of cellulases with cellulose films.

Manipulating the contrast between various components is integral to neutron scattering approaches. For organic materials, this is readily accomplished using the very different neutron scattering properties of hydrogen and deuterium. Often, measurements in aqueous environments are made using D_2O rather than H_2O to enhance contrast, decrease the incoherent background that arises mainly from protons in the sample, and increase the signal-to-noise (decrease the counting time). However, care must be taken when labile protons are present in the sample because H/D exchange must be taken into account in the analysis. Therefore, prior to the digestion studies, we performed a comparison of the swelling of cellulose films in both D_2O and H_2O buffer.

We first compare the swelling behavior of amorphous cellulose films in D_2O and in H_2O. Then, we report results for film digestion in H_2O buffer by a commercial fungal extract from *T. viride* consisting of a large number of enzymes of various types[20] and by an endoglucanase from *A. niger*.

MATERIALS AND EXPERIMENTS

Sodium hydroxide, acetic acid, microcrystalline cellulose (Avicel PH-101), hexamethyldisilazane, dimethylacetamide, lithium chloride, tetrahydrofuran, and methanol were all purchased from Sigma Aldrich. (Certain trade names and company products are identified to specify adequately the experimental procedure. In no case does such identification imply a recommendation or endorsement by the National Institute of Standards and Technology, nor does it imply that the products are necessarily the best for the purpose.) D_2O (99%) was purchased from Cambridge Isotopes. The commercial cellulase extract from *Trichoderma viride* was purchased from Sigma-Aldrich (C9422-5KU). The GH12 endoglucanase from *A. niger* was obtained from Megazyme as the product CelAN. It runs as a single band on SDS-PAGE with molecular weight of 27 kDa. *T. viride* was dissolved in 50 mM sodium acetate buffer pH 5.0. CelAN was dissolved in 50 mM sodium acetate buffer pH 4.5.

Preparation of Regenerated Cellulose Films. Smooth, uniform regenerated cellulose films were prepared on polished silicon wafers (diameter = 75 mm, thickness = 5 mm) and on QCM-D sensors (diameter = 14 mm and thickness = 0.3 mm) from precursor films of trimethylsilylcellulose (TMSC). TMSC was prepared from microcrystalline cellulose, as reported elsewhere.[16,21] The QCM sensors consisted of a quartz crystal covered with 5 nm of chromium and 100 nm of gold. They were cleaned via an UV/ozone ProCleaner (Bioforce Nanoscience) for 10 min and boiled in a 1:1:5 by volume solution of conc. ammonium hydroxide/30% by volume hydrogen peroxide/water for 0.5 h. The sensors were then rinsed exhaustively with ultrapure water prior to spincoating TMSC. The polished silicon wafers for NR were cleaned with piranha (conc. sulfuric acid/30% by volume hydrogen peroxide, 7:3 by volume), followed by UV/ozone treatment for 20 min. TMSC was spincoated onto the cleaned substrates with spinning speeds ranging from 2000 to 4000 rpm from toluene solutions ranging in concentration from 10 to 18.0 $g \cdot L^{-1}$. To minimize surface roughness for the NR samples, we typically filtered the TMSC solution through a 1.0 μm syringe filter as the solution was deposited onto the wafer for spin-coating. After the substrates were spincoated, residual toluene was removed by heating the samples under vacuum. Trimethylsilyl groups were cleaved by brief exposure of the TMSC-coated substrates to the vapors of an aqueous HCl solution as previously reported.[16,22] Highly smooth films are essential for maximizing the information obtainable from NR. Whereas the dry films in air were typically very smooth, the smoothness of the films upon swelling was highly dependent upon the concentration of the HCl solution used for conversion of TMSC to cellulose. The TMSC films used for the NR studies were converted to cellulose by exposure to vapors from 0.5 N HCl solution in a closed container for 15 min. Converting the films using higher concentrations of HCl and lower time resulted in increased interfacial roughness (Supporting Information, Figure S1). IR spectra (Supporting Information, Figure S2) indicated complete conversion of TMSC to cellulose. No diffraction peaks were present for these films when analyzed by grazing incidence X-ray diffraction (Supporting Information, Figure S3), as previously reported by others.[23]

The thicknesses of regenerated cellulose films on the QCM-D. substrates were determined by angle-resolved laser (632.8 nm, He−Ne laser) ellipsometry (Picometer Ellipsometer, Beaglehole Instruments, Wellington, New Zealand). The data were collected in 1.0° intervals from 65 to 80°. Measurements were made at three spots, and reported values were the average with one standard deviation error bar. For the NR samples, the dry film thicknesses were determined from X-ray reflectivity (XR) and NR. Film thicknesses ranged from 240 to 310 Å. This range of thicknesses resulted as conditions (solution concentration, spinning speed and acceleration, extent of repeated filtration, and filter size) were varied in an attempt to minimize the surface roughness. XR scans are shown in Figure S1 (Supporting Information) for samples regenerated from TMSC films that were spun from a 10 mg/mL in toluene.

Neutron Reflectivity. In NR, one measures the ratio of reflected to incident intensity as a function of momentum transfer $q_z = (4\pi/\lambda) \sin \theta$,

where θ is the angle of incidence with respect to the plane of the film and λ is the wavelength.[19] The form of this curve is determined by the in-plane averaged scattering length density (SLD also denoted b/v) profile normal to the surface. The SLD is directly related to the atomic composition and the density.[19] NR studies were performed on the SPEAR reflectometer (Lujan Center/LANSCE) and the liquids reflectometer (SNS/ORNL). Both reflectometers operate in the time-of-flight mode where a band of wavelengths impinge onto the sample and are resolved at the detector based on their time-of-flight. Data collected for several angles were merged together to create the full curves. In some cases, repeated scans were performed at a single angle to follow more rapid changes with time. In that case, the duration of each NR scan was 30 min. For the measurements, a silicon wafer coated with regenerated cellulose was placed in a solid−liquid cell. The neutron beam impinged onto the film/buffer interface by passing through the silicon wafer. The regenerated cellulose films were allowed to equilibrate with sodium acetate buffer for 20 min, after which several scans were collected. Then, 2 to 3 mL of enzyme solution was injected into the cell, and scans were performed in the absence of flow until no further change was detected. The measurements were performed at 20 °C.

Whereas NR measurements performed in H_2O have the advantage of avoiding the complicating effects of H/D exchange, they have the disadvantage that the reflectivity data do not possess a total reflection edge because the SLD of H_2O is less than that of silicon. This is particularly problematic for reflectometers at spallation sources operating in the time-of-flight mode. To put the reflectivity data on an absolute scale, a data set for a cellulose film swollen in H_2O was adjusted by a multiplicative factor until the best fit was obtained using a simple model involving one or two layers for the cellulose film and the known thickness and SLD of the silicon oxide. Plots of reduced χ^2, indicating the quality of the fit, versus the multiplicative factor consistently gave a well-defined minimum, as shown in Figure S4 (Supporting Information). The rest of the data sets were then scaled to the reference data set using the monitor counts or the total beam current on the sample. This method was validated by collecting NR data for a swollen cellulose film on the NG1 reflectometer (NCNR, NIST) that employs a monochromatic incident beam selected from the output of a reactor source such that absolute reflectivity is obtained to ±5%. In that case, the normalization achieved through the fitting procedure describe above was in excellent agreement with the absolute reflectivity. From data such as that in Figure S4 of the Supporting Information, we estimate a ±10% uncertainty in the absolute reflectivity values. This level of uncertainty does not affect any conclusions of this study.

The NR data were analyzed using the Ga_refl program[24] based on the Parratt recursive formalism.[25] Simultaneous fits of the NR data were performed for all data sets at different stages of a single adsorption run. Simultaneous analysis allowed particular characteristics to be maintained constant for all fits, in particular, the SLD of the buffer solution and the SLD and roughness of the silicon oxide layer. In all cases, the fits included only the minimum number of layers that were required to achieve a good fit to the data. In the Ga_refl program, the roughness parameter is the full width at half-maximum (fwhm = 2.35 σ, where σ is the standard deviation) of a Gaussian distribution and was constrained in the fitting to be less than the smallest thickness of the two adjacent layers.

Fitting reflectivity data results in defining a family of SLD curves that are consistent with the data. The uncertainty in the fitted profiles was determined by a Monte Carlo resampling procedure[26] in which a large number (1000) of statistically independent sets of reflectivity data were created from the original data set and the uncertainty from the counting statistics. Each set of reflectivity data was analyzed using the fitting procedure described above. The result is a range of values for each fitting parameter that is consistent with the statistics of the original data. This results in SLD profile bands. The reported uncertainties of particular parameter values correspond to 2σ confidence intervals, where σ is the standard deviation of the distribution.

The volume fraction of cellulose was determined from the measured SLD of the swollen film and the SLD values of the buffer solution and pure cellulose using the following relation (assumes additivity of volumes)

$$(b/v)_{\text{meas}} = \phi_{\text{cellulose}}(b/v)_{\text{cellulose}} + (1 - \phi_{\text{cellulose}})(b/v)_{\text{buffer}} \quad (1)$$

where $(b/v)_{\text{meas}}$ is the measured SLD for the swollen film, $\phi_{\text{cellulose}}$ is the volume fraction of cellulose, $(b/v)_{\text{cellulose}}$ is the SLD of pure cellulose ($C_6H_{10}O_5$), and $(b/v)_{H_2O\ \text{buffer}} = -0.54 \times 10^{-6}$ Å^{-2} and $(b/v)_{D_2O\ \text{buffer}} = 6.35 \times 10^{-6}$ Å^{-2} are the SLD values for H_2O buffer and D_2O buffer, respectively. In D_2O buffer, the three labile protons per repeat unit of cellulose will rapidly exchange with deuterons from the buffer.[27] In that case, the SLD of pure cellulose with composition $C_6H_7D_3O_5$ must be used in eq 1. The SLD values for $C_6H_{10}O_5$ and $C_6H_7D_3O_5$ used in our calculations were 1.67×10^{-6} and 3.39×10^{-6} Å^{-2}, respectively, as discussed in the Results section.

QCM-D. An E4 quartz crystal microbalance (Q-Sense AB) was used to investigate the adsorption and activity of the enzymes on regenerated cellulose films. The QCM-D sensor coated with a regenerated cellulose film was placed in a flow cell. The regenerated cellulose film was allowed to equilibrate for 1 h in sodium acetate buffer to obtain a flat baseline. Then, 1.0 mL of enzyme solution was injected into the flow cell. Measurements were made in the absence of flow. Frequency (Δf) and dissipation (ΔD) changes for the fundamental frequency (4.95 MHz for gold coated quartz crystals) and six odd overtones ($n = 3$ - 13) were monitored simultaneously. At the end of the measurement, sodium acetate buffer was typically flowed through the system for the removal of residual and reversibly adsorbed enzyme and products. Normally, Δf and ΔD from the first overtone were noisy because of insufficient energy trapping. Thus, the adsorption curves from the third overtone ($n = 3$) are shown in the graphs.

For QCM-D measurements, if the adsorbed mass is evenly distributed, rigidly attached, and small compared to the mass of the crystal, Δm, mass per unit area, can be calculated by the Sauerbrey equation[28]

$$\Delta m = -\frac{C\Delta f}{n} \quad (2)$$

where n is the overtone number and C is a constant (0.177 mg·m^{-2}·Hz^{1-}). However, the linear relationship between the adsorbed mass and the frequency change is not valid for viscoelastic layers adsorbed onto the solid surfaces. By measuring the dissipation of energy in the adsorbed layers simultaneously with the frequency change, information is obtained about the rigidity/softness of the adsorbed layer. The dissipation factor is defined as a ratio between the energy dissipated and the energy stored during a single oscillation[28]

$$D = \frac{E_{\text{dissipted}}}{2\pi E_{\text{stored}}} \quad (3)$$

X-RAY REFLECTION AND GRAZING INCIDENCE X-RAY DIFFRACTION

X-ray reflectivity (XR) measurements were performed using a Scintag X_1 powder diffractometer equipped with Cu Kα radiation, an incident beam mirror, and a Peltier-cooled solid-state Ge detector. An incident beam mirror was used to generate a parallel beam (in the height dimension) from the divergent X-ray source. A variable slit system at the exit port of the mirror housing was adjusted to create a beam of 50 μm in height. The beam width was 10 mm. Two slits in front of the detector were used to reduce background scattering and limit the beam divergence.

Grazing incidence X-ray diffraction of film specimens was performed using a Siemens D500 $\theta-2\theta$ diffractometer employing a sealed tube Cu Kα radiation source. Incident beam optics employed 0.3° divergence and antiscatter slits which bracketed a set of soller slits (to reduce axial divergence). The diffracted beam optics consisted of a long soller slit optic (length = 15 cm, 0.4° divergence), a diffracted-beam LiF monochromator, and a scintillation detector. Grazing incidence angles were typically between 0.5 to 2.0° and scan parameters were 5−40° 2θ angular range, 0.04° step size, and 25 s count time.

INFRARED SPECTROSCOPY

Infrared (IR) spectra for TMSC and regenerated cellulose films on polished silicon wafers were obtained in reflectance mode, using an IR microscope (Nicolet Continuum model 912A0429) with a sampling aperture of 100 μm × 100 μm and a Nicolet Nexus 870 Fourier transform infrared spectrometer.

RESULTS

NR Studies. *Cellulose Films in Air and in H_2O and D_2O.* NR data for an amorphous cellulose film in air and swollen with H_2O buffer are shown in Figure S5 (Supporting Information). Many strong fringes are present to q_z values greater than 0.06 Å^{-1}. These fringes are due to constructive and destructive interferences. The spacing of the fringes is inversely proportional to the film thickness, and the magnitude of the fringes is determined by the difference in SLD between the film and the surrounding medium (air in this case). Interfacial roughness dampens the fringes with increased intensity at higher q_z values. The SLD of the amorphous cellulose films in air was typically ∼1.5 × 10^{-6} Å^{-2} corresponding to a calculated density of 1.28 g/cm^3. This SLD value is in agreement with a value previously reported by another group for the same film preparation method.[23] Values reported in the literature for the density of amorphous cellulose range from 1.27 to 1.5 g/cm^3.[29−32] For comparison, the density of crystalline cellulose is ∼1.6 g/cm^3,[30,33] and the SLD is 1.87 × 10^{-6} Å^{-2}. The film thickness increased from 303 Å in air to 473 ± 5 Å upon swelling in water, corresponding to an increase by a factor of ∼1.6. Throughout the course of this work, the swelling factor in H_2O ranged from 1.6 to 2.1 for different samples. A swelling factor of 2.0 has been reported elsewhere for cellulose films of thickness 200 Å in air.[23] In determining the volume fraction of water within the swollen films using eq 1, there is some ambiguity as to the SLD value most appropriate to use for pure cellulose. The specific volume differs by 20% between amorphous and crystalline cellulose, and to our knowledge, the volume excluded to water by cellulose chains in the amorphous film is unknown. Use of the SLD of amorphous cellulose (1.5 × 10^{-6} Å^{-2}) in eq 1 resulted in a calculated volume fraction cellulose ($\phi_{cellulose}$) in the majority of the film of 0.54. Integrating the profile of $\phi_{cellulose}$ yielded 253 Å, which is 9% higher than the value of 233 Å obtained from integrating the profile of $\phi_{cellulose}$ for the dry film (Figure S5e of the Supporting Information). Use of the SLD of crystalline cellulose (1.87 × 10^{-6} Å^{-2}) in eq 1 resulted in a calculated $\phi_{cellulose}$ in the majority of the film of 0.45. Integrating the profile of $\phi_{cellulose}$ yielded 213 Å, 13% lower than the value obtained for the dry film. Agreement in the total amount of cellulose between the swollen and dry film measurements was obtained with an SLD for cellulose of 1.67 × 10^{-6} Å^{-2}, which lies in between the values for the crystalline and amorphous states. This SLD value, corresponding to a density of 1.48 g/cm^3, was used to calculate the volume fraction values for all measurements in H_2O.

For the various samples studied in this work, the swelling was fairly uniform through the thickness of the films, although, in many cases, including an additional layer or two with slightly different SLD at the substrate surface significantly improved the fit. Variation in SLD near the substrate could be explained by variable water swelling due to molecular confinement, incomplete conversion of TMSC to cellulose in the molecular layers immediately adjacent to the substrate, or variation in adhesion of the first molecular layers to the native silicon oxide. These variations could result from small differences in the film preparation protocol. The effects could also be only apparent, resulting instead from small errors in splicing together the NR data from different incident angles. Full characterization of this effect would require many repeated runs and higher resolution data than obtained in this study and is not the focus of this work. Variability in the SLD profiles near the substrate surface does not affect any conclusions of this study, which focuses on the digestion of the films by enzymes adsorbing at the solution−film interface.

NR curves for a cellulose film swollen with H_2O and with D_2O are given in Figure 1. In this case, NR data were collected for a series of conditions in which the film was first swollen in pure H_2O, then in H_2O buffer (50 mM Na acetate pH 5), then pure D_2O, then again in the same in H_2O buffer. The three curves involving H_2O and H_2O buffer were indistinguishable (Supporting Information, Figure S6). This shows that the extent of swelling in H_2O and in H_2O buffer is identical and also that H/D exchange upon switching between H_2O and D_2O is rapidly reversible. For the film swollen with D_2O, an SLD of 3.39 × 10^{-6} Å^{-2} was used for $C_6H_7D_3O_5$ corresponding to a density of 1.48 g/cm^3 to calculate $\phi_{cellulose}$ in the film. The data in Figure 1 indicate that the water volume fraction and the film thickness were both slightly greater with D_2O than with H_2O. This was a consistent finding in several trials. For the data in Figure 1, ϕ_{D_2O} of the majority layer was 0.59 ± 0.01, whereas ϕ_{H_2O} of the majority layer was 0.56 ± 0.01. The total thickness of the swollen film in each case was 592 ± 3 Å (D_2O) and 575 ± 3 Å (H_2O). D_2O and H_2O are known to have slightly different thermodynamic properties and hydrogen bonding characteristics due to the difference in the polarizability of OH and OD bonds.[34−36] The value of ϕ_{D_2O} reported here is much lower than the reported recently by Kontturi et al (0.89).[23] Whereas the films in their work were thinner and may swell to a greater extent than the present films, we believe that the difference in ϕ_{D_2O} is primarily due to H/D exchange that was neglected in the prior work.

Studies of Enzymatic Digestion. *T. viride Extract.* Results for 0.3 mg/mL *T. viride* in H_2O buffer are shown in Figure 2. Because the extract is a complex mixture of enzymes,[20] a precise molar concentration cannot be determined. Assuming an average molecular weight of 60 kDa, 0.3 mg/mL corresponds to 5 μM. Upon injecting the enzyme extract, the fringes shift to higher q_z values, with a slight increase in spacing, indicating a decrease in the thickness of the film. The fringes rapidly decrease in magnitude and become strongly damped at higher q_z values such that only one weak fringe remained in the scan initiated 1 h after injecting the enzyme extract. The SLD profile bands, indicating 95% confidence intervals from a Monte Carlo error analysis,[26] are given in Figure 2b. The volume fraction profiles bands are given in Figure 2c. Initially, the main effect was a decrease in the thickness of the film and substantially increased roughness at the solution/film interface. This indicates that the enzymes are most

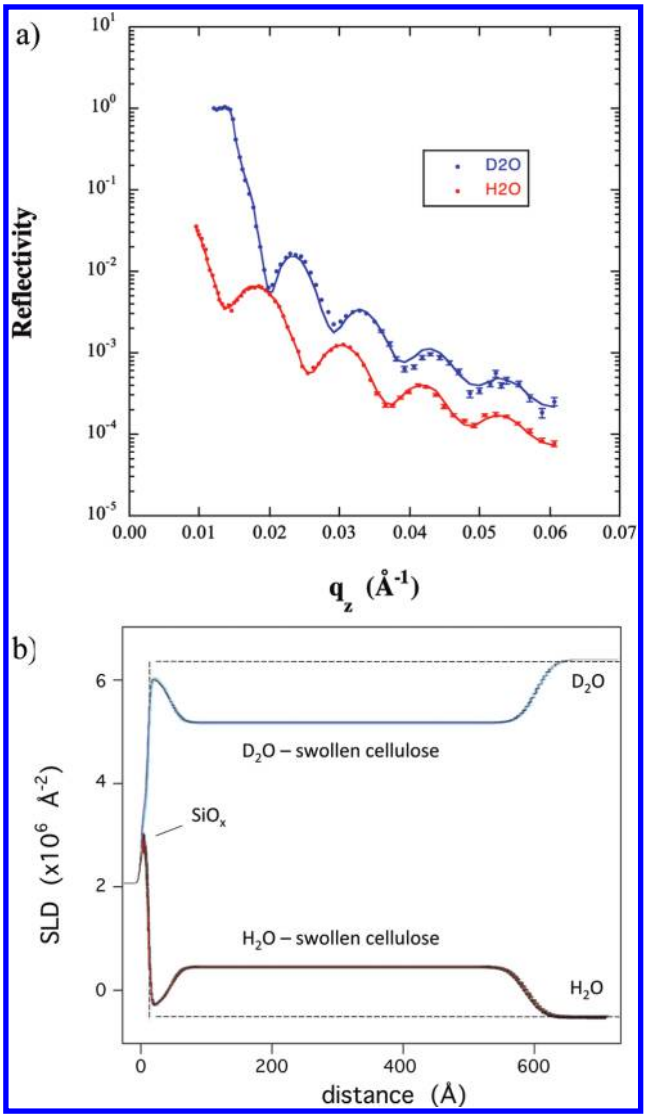

Figure 1. (a) NR data for a 280 Å regenerated cellulose film swollen in D_2O and H_2O. (b) SLD profile bands from simultaneous fits to the data in part a.

active at the outer surface of the film and that the initial activity creates a topologically rough interface. However, for the scan initiated 1 h after the enzyme extract was injected, increased water content within the bulk of the film is apparent, which indicates that the enzymes began to penetrate and digest within the bulk of the film. After 4.5 h, almost no cellulose remained. In that case, the reflectivity data are only slightly below the calculated curve for a bare silicon wafer with native oxide layer (Figure S7, Supporting Information). Similar results were obtained at 1 mg/mL *T. viride*, although in that case, digestion of the film occurred at an elevated rate (Figure S8, Supporting Information).

CelAN. NR data for CelAN at 5.0 μM and 20 °C are shown in Figure 3. NR data collected 12.5 h after injecting CelAN are compared with data for pure buffer in Figure 3a, and volume fraction profiles bands are given in Figure 3b. After 12.5 h, the fringes have shifted to higher q_z, indicating a decrease in film thickness. However, the magnitude of the fringes decreased only slightly, and the fringes were not damped at higher q_z as was the case with the *T. viride* extract. In fact, after 4.5 days (Figure S9, Supporting Information), the fringes remained at nearly the same magnitude as for the data after 12.5 h in Figure 3b. The volume fraction profile bands in Figure 3b show that the film thickness decreased ~30 Å within the first 12.5 h, whereas the water volume fraction within the film either remained the same or increased only slightly (from 0.60 ± 0.03 to 0.64 ± 0.04). No increase in the roughness of the film−solution interface was observed, in contrast with the data for *T. viride*. Integration of the volume fraction profiles in Figure 3c indicates that 16 ± 2% of the cellulose mass was lost from the film. Short (30 min) scans in which data were collected over a more limited q_z range were repeated during the first several hours after injecting CelAN. Two such scans, initiated 0.5 and 3.0 h after injecting CelAN, are shown in Figure 4a. The volume fraction profile bands from the scan at 3.0 hr and the scan prior to adding enzymes. are shown in Figure 4b. Whereas the uncertainty is larger because of the limited q_z range, the results indicate that initially CelAN is active mainly at the surface.

QCM Studies. *T. viride.* Results for *T. viride* exposed to 300 Å regenerated films at 1 and 0.3 mg/mL are shown in Figure 5. Data are shown for the third overtone (n = 3) only, as little variation was observed for different overtones. The results are qualitatively similar for the two concentrations. ($\Delta f/n$) decreased immediately upon injection of enzymes because of adsorption and then increased gradually as mass was released from the film. A plateau was reached when nearly all cellulose was digested. The plateau was reached in 4 to 5 h for 1 mg/mL and >7 h for 0.3 mg/mL. In each case, ΔD increased to a maximum and then decreased. These features are similar to those previously reported for digestion of amorphous cellulose films using a different fungal extract (*Trichoderma reesei*).[5] The increase in dissipation occurs as the bulk of the film becomes more viscoeleastic. Initially, the dissipation increases slowly, but an increase in slope occurs as the dissipation increases toward the maximum. We speculate that the weaker slope in the earlier stage corresponds to digestion from the surface of the film (stiffness of the majority of the film largely unchanged), and the stronger slope indicates penetration of enzyme into and digestion within the bulk of the film, decreasing the stiffness throughout the bulk of the film. A maximum was reached, and then the dissipation decreased as the mass in the film became depleted.

CelAN. Results for CelAN at 5.0 μM in contact with a 242 Å regenerated cellulose film are shown in Figure 6. The results are qualitatively different from the results for the *T. viride* extract. Following the adsorption phase in which a sharp drop in ($\Delta f/n$) and a small increase in ΔD were observed, ($\Delta f/n$) increased only very gradually over 15 hours, and virtually no change was observed in ΔD. Little variation with overtone was observed. Because no change in dissipation occurred, the change in mass can be estimated using the Sauerbrey equation. The increase in $\Delta f/n$ observed after 15 h corresponds to a loss of 117 ng/cm^2.

DISCUSSION

NR and QCM-D are highly complementary and can reveal important new insight into the actions of cellulases on amorphous cellulose films. In this work, we performed the NR studies using H_2O buffer rather than D_2O buffer to avoid complications in the quantitative interpretation of the SLD profiles due to H/D exchange and also because the kinetics of enzymatic reactions may be affected by the difference in the polarizability of OH and OD bonds. The time scale of the changes in the QCM-D and NR data cannot be compared quantitatively because in the absence of flow, the hydrolysis rates depend strongly on the geometry of the

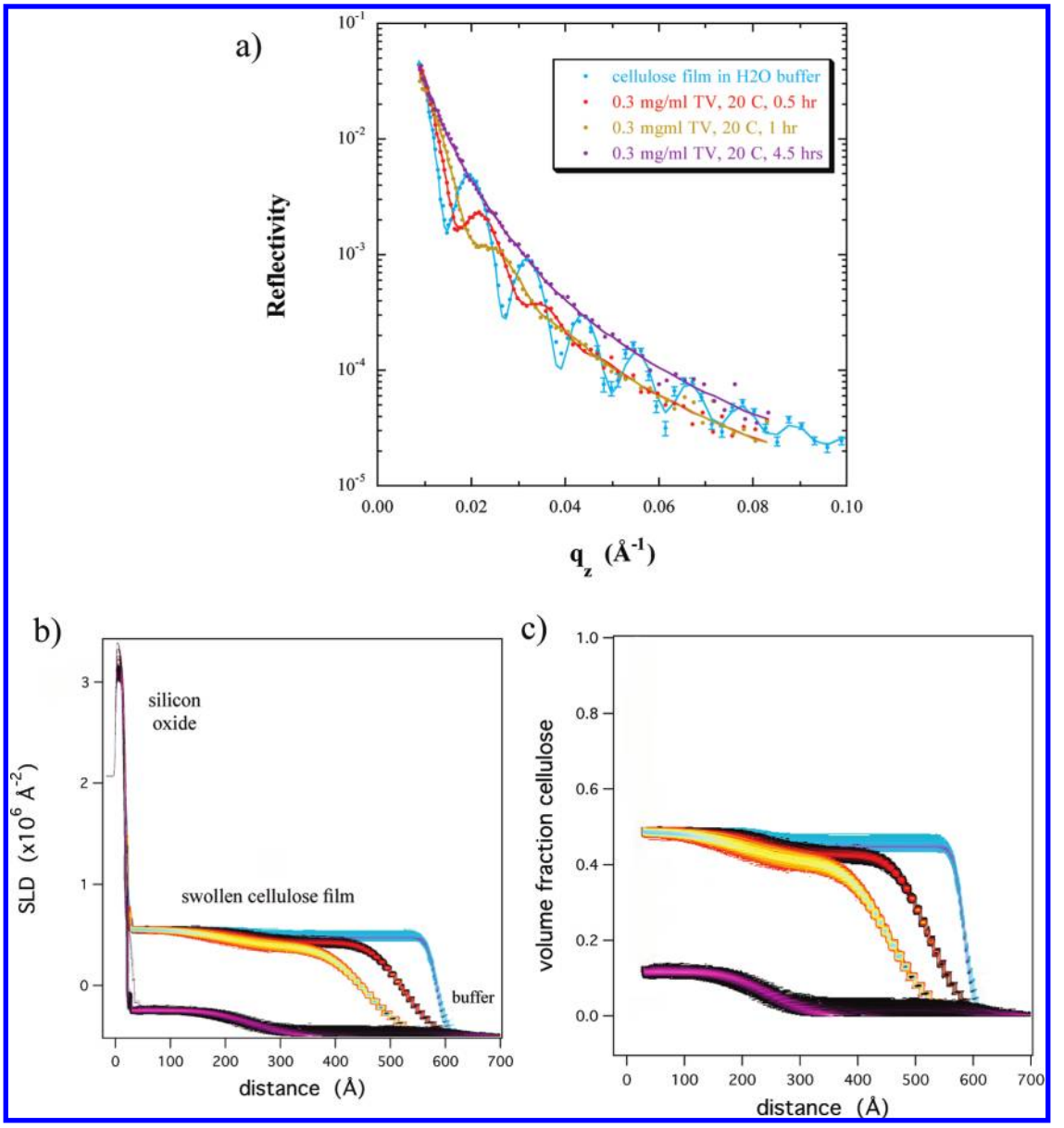

Figure 2. (a) NR data for a 280 Å regenerated cellulose film exposed to a solution of *T. viride* extract at 0.3 mg/mL and 20 °C. SLD profile bands and cellulose volume fraction profiles from the fitting analysis are shown in parts b) and c), respectively.

sample cells, which differ between the two techniques. Presumably, this is due to differences in the rates of convection within the cells. In fact, we have observed large differences in rate as a function of sample geometry (channel depth and width) in studies using cells made from a glass slide and coverslip joined by an adhesive gasket. Therefore, in the following we compare the qualitative trends in the data between the two techniques rather than comparing the data quantitatively at specific time points. We also note that without deuterium enrichment of the enzymes, the NR measurement is largely insensitive to the presence of adsorbed enzyme. Therefore, in this study QCM-D alone provides information about the amount of adsorbed enzyme. This is reflected by the magnitude of the initial drop in $(\Delta f/n)$ upon injection of enzyme. Because adsorption of enzyme would slightly increase the neutron SLD, the cellulose (water) volume fraction values calculated from the NR data are actually upper (lower) limits.

Digestion by *T. viride* Extract and CelAN. A QCM-D study of digestion of cellulose films by commercial enzymes has been previously reported,[5] but the present work is the first that involves NR. Both NR and QCM-D show that the *T. viride* extract at 0.3 mg/mL removes nearly the entire film within a few hours at 20 °C. The NR data are consistent with the model of film digestion previously proposed by Turon et al.[5] Initially, NR shows that the enzymes release mass from the outer surface of the film. This is consistent with the initially weak slope in the dissipation curve from QCM-D. Substantial roughening of the film−solution interface occurs in the earliest stage. After several hours, increased water content was present within the bulk of the film and additional mass was released from both the surface and the bulk of the film. This correlates with the increase in slope in the dissipation curve in QCM-D prior to reaching the maximum. The roughness of the film−solution interface continued to increase. At no point was there an increase in the thickness of

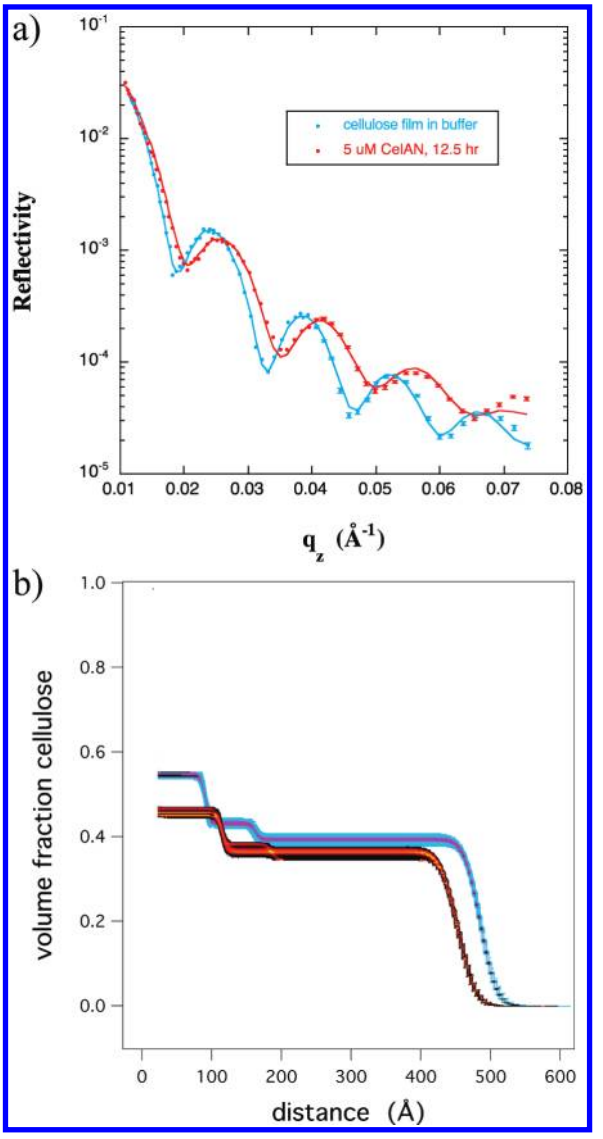

Figure 3. (a) NR data for a 240 Å regenerated cellulose film exposed to a solution of CelAN at 5.0 μM and 20 °C. Volume fraction profile bands from the fitting analysis are shown in part b). The red/black color scheme corresponds to the data after 12.5 h of digestion.

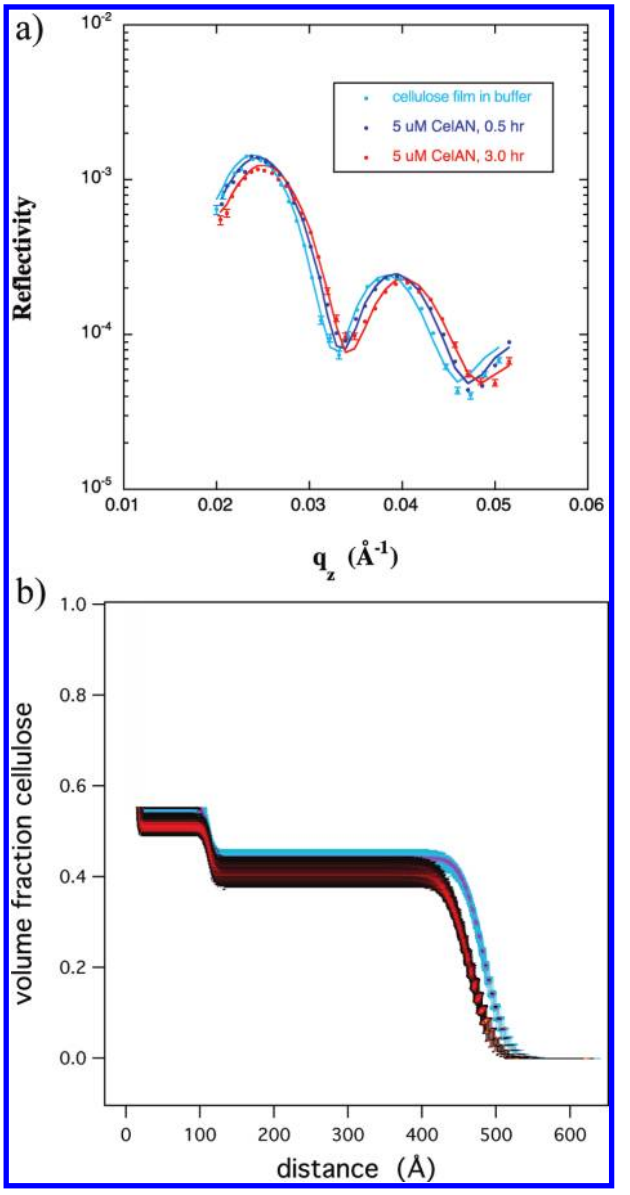

Figure 4. (a) NR data (short scans) for the same sample as in Figure 3. Volume fraction profile bands for buffer only and for the scan initiated at 3.0 h are shown in part b). The red/black color scheme corresponds to the scan initiated 3.0 h after introducing the enzyme.

the film (taken as the distance from the substrate to the midpoint of the solution/film interface in Figure 2), only a steady decrease in thickness. A prior QCM-D study involving cellulose II films anchored to silicon oxide surfaces suggested that some fungal endoglucanases result in film swelling.[13]

The NR data for CelAN show distinctly different behavior than for the *T. viride* extract. The data indicate that at 20 °C this enzyme is active primarily at the surface of the film. Even after 12.5 h, very little penetration into the film is evident, as the water content increased only slightly from 60 to 64%. In addition, as seen in Figure 3b, the roughness at the film/solution interface did not change detectably in 12.5 h. The QCM-D results show virtually no increase in dissipation and only a small gradual increase in $(\Delta f/n)$ over that time period. The lack of change in dissipation is consistent with little change in the mechanical properties of the bulk film, whereas the small increase in $(\Delta f/n)$ is consistent with a low level of mass released at the surface of the film.

The loss of 117 ng/cm^2 after 15 h as determined from the QCM-D data suggests that the amount of cellulose released as soluble sugars was lower in that case than in the NR study. The initial dry film thickness of 242 Å with density 1.28 g/cm^3 corresponds to 3098 ng/cm^2 of cellulose, so we estimate ~4% of the cellulose mass was released in the QCM study of CelAN. This is considerably lower than the 16% loss observed in the NR study. We note that the loss of bound water as cellulose is released from the surface of the film also contributes to the increase in $\Delta f/n$, but this effect is partially compensated by the fact that a small amount of cellulose mass is released from the bulk of the film and is replaced by water. From the volume fraction profile in Figure 3b, the amounts of water lost at the surface and gained within the bulk of the film are roughly comparable. Therefore, the difference in cellulose mass released in the two studies appears to be outside the uncertainty. We attribute the difference to the very

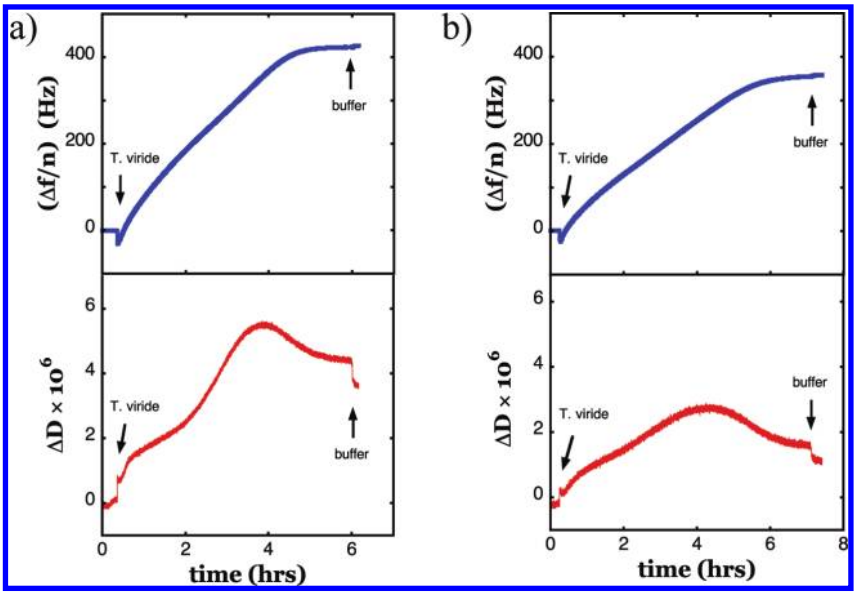

Figure 5. ($\Delta f/n$) and ΔD versus time from QCM-D for 300 Å regenerated cellulose films exposed to solutions of *T. viride* extract at (a) 1 and (b) 0.3 mg/mL at 20 °C. Curves correspond to the third overtone. Arrows indicate where solutions were switched.

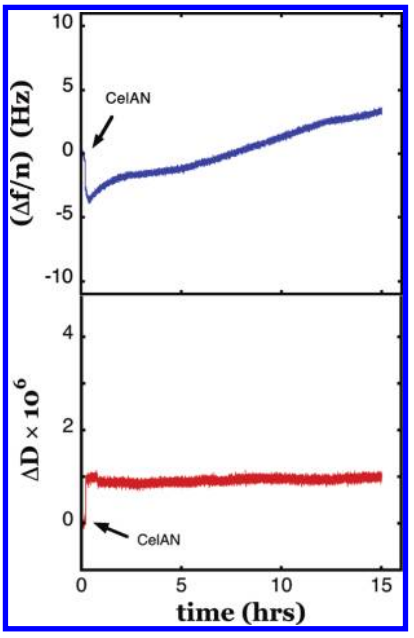

Figure 6. ($\Delta f/n$) and ΔD versus time from QCM-D for a 240 Å regenerated cellulose film exposed to 5.0 μM CelAN at 20 °C. Curves correspond to the third overtone.

different sample geometries and therefore different rates of convection within the sample cells. Unfortunately, it is not currently feasible to perform NR and QCM-D on samples of similar size as is the case with optical techniques such as ellipsometry and surface plasmon resonance.[37]

The fact that the *T. viride* extract penetrated and digested within the cellulose film whereas on the same time scale CelAN was active only at the surface is most likely due to the actions of exoglucanases in the *T. viride* extract and possibly also to the presence of cellulose binding domains on the enzymes in the *T. viride* extract. CelAN does not contain a cellulose binding domain.

The sequence of changes observed in the NR data in Figure 2 and Figure S8 of the Supporting Information provides some insight into the actions of the enzymes in the *T. viride* extract. The cellulase of *T. viride* is known to contain six endoglucanases and three exoglucanases.[20] Whereas the enzymes of *T. viride* initially digested at the surface, as for the endoglucanase CelAN, the *T. viride* cellulase rapidly roughened the film/solution interface, which was not seen for CelAN. We postulate that the interfacial roughening is due to the actions of the exoglucanases. Enzyme activity within the bulk of the film occurs only after a significant fraction of the upper layer is degraded. Such an inhomogeneous layer would make viscoelastic modeling of the QCM-D data extremely difficult.[38]

CONCLUSIONS

QCM-D and NR are highly complementary and provide unprecedented insight into the effect of cellulases on the structure of cellulose films. QCM-D provides changes in mass and in film stiffness whereas NR reveals the profile of water through the film at nanometer resolution and is highly sensitive to interfacial roughness. Prior to studies of digestion, swelling studies were performed in D_2O and in H_2O. Substantial H/D exchange occurs upon exposure of cellulose films to D_2O. The degree of swelling (both the volume fraction of water and film thickness increase) is slightly greater for D_2O than for H_2O. No difference in swelling was detected between pure H_2O and H_2O buffer (50 mM Na acetate pH 5). The results for digestion by a fungal enzyme extract and for a single endoglucanase show that these techniques can reveal important differences in the interactions of the enzymes with the films. In particular, the endoglucanase was only active at the surface and did not lead to roughening of the interface, whereas the full enzyme extract first roughened the surface and then penetrated and digested within the bulk of the film. Additional insight is certain to come from future studies involving these techniques.

ASSOCIATED CONTENT

Supporting Information. X-ray reflectivity from dry cellulose films regenerated from TMSC. Plot of FTIR data for

TMSC film as deposited and after exposure to vapors of 0.5 N HCl solution for 5 and 10 min. Grazing incidence diffraction data for a cellulose film regenerated from TMSC. Sample plot of χ^2 versus normalization factor for fits to NR data of a cellulose film in H_2O buffer. NR data and SLD profile for cellulose film in air and in H_2O buffer along with resulting volume fraction profile. Comparison of NR data for cellulose film in H_2O, H_2O buffer and in H_2O buffer after having exchanged to D_2O. Comparison of NR data after 4.5 h of digestion with 0.3 mg/mL *T. viride* with the calculated curve for bare silicon oxide. Time-resolved NR data for 1.0 mg/mL *T. viride* in H_2O buffer. NR data for regenerated cellulose film exposed to a solution of CelAN at 5.0 μM for 4.5 days. This material is available free of charge via the Internet at http://pubs.acs.org.

AUTHOR INFORMATION

Present Addresses

[○]DuPont (China) R&D Center, Shanghai, China.

ACKNOWLEDGMENT

This work was part of the DOE Joint BioEnergy Institute (http://www.jbei.org) supported by the U.S. Department of Energy, Office of Science, Office of Biological and Environmental Research, through contract DE-AC02-05CH11231 between Lawrence Berkeley National Laboratory and the U.S. Department of Energy. The research at the Los Alamos Neutron Science Center and the Spallation Neutron Source at Oak Ridge National Laboratory was sponsored by the Scientific User Facilities Division, Office of Basic Energy Sciences, U.S. Department of Energy under DOE contracts DE-AC52-06NA25396 and DE-AC05-00OR22725. Sandia is a multiprogram laboratory operated by Sandia Corporation, a Lockheed Martin Company, for the United States Department of Energy under contract DE-AC04-94AL85000. We acknowledge the support of the National Institute of Standards and Technology, U.S. Department of Commerce, in providing the research facilities at NCNR. A.R.E., Z.L., and C. W. were supported as part of the Center for LignoCellulose Structure and Formation, an Energy Frontier Research Center funded by the U.S. Department of Energy, Office of Science, Office of Basic Energy Sciences under award number DE-SC0001090. We wish to thank Frank Heinrich for providing the code used to perform the Monte Carlo resampling procedure in the analysis of the NR data.

REFERENCES

(1) Somerville, S.; Young, H.; Taylor, C.; Davis, S. C.; Long, S. P. *Science* **2010**, *13*, 790–792.

(2) Samayam, I. P.; Schall, C. A. *Bioresour. Technol.* **2010**, *101*, 3561–3566.

(3) Laureano-Perez, L.; Teymouri, F.; Alizadeh, H.; Dale, B. E. *Appl. Biochem. Biotechnol.* **2005**, *124*, 1081–1099.

(4) Liu, W.; Zhang, X. Z.; Zhang, Y. H. P. *Appl. Environ. Microbiol.* **2010**, *76*, 4914–4917.

(5) Turon, X.; Rojas, O. J.; Deinhammer, R. S. *Langmuir* **2008**, *24*, 3880–3887.

(6) Sun, N.; Rahman, M.; Qin, Y.; Maim, M. L.; Rodriquez, H.; Rogers, R. *Green Chem.* **2009**, *11*, 646–655.

(7) Simmons, B. A.; Singh, S.; Holmes, B. M.; Blanch, H. W. *Chem. Eng. Process.* **2010**, *106*, 50–55.

(8) Cheng, G.; Varanasi, P.; Li, C.; Liu, H.; Melnichenko, Y.; Simmons, B. A.; Kent, M. S.; Singh, S. *Biomacromolecules* **2011**in press.

(9) Dadi, A. P.; Varanasi, S.; Schall, C. A. *Biotechnol. Bioeng.* **2006**, *95*, 904–910.

(10) Laureano-Perez, L.; Teymouri, F.; Alizadeh, H.; Dale, B. E. *Appl. Biochem. Biotechnol.* **2005**, *124*, 1081–1099.

(11) Kumar, R.; Mago, G.; Balan, V.; Wyman, C. E. *Bioresour. Technol.* **2009**, *100*, 3948–3962.

(12) Wood, T. M. *Methods Enzymol.* **1988**, *160*, 19–25.

(13) Josefsson, P.; Henriksson, G.; Wagberg, L. *Biomacromolecules* **2008**, *9*, 249–254.

(14) Vuong, T.; Wilson, D. B. *Appl. Environ. Microbiol.* **2009**, *75*, 6655–6661.

(15) Bhat, M. K.; Bhat, S. *Biotechnol. Adv.* **1997**, *15*, 583–620.

(16) Kontturi, E.; Thune, P. C.; Niemantsverdriet, J. W. *Langmuir* **2003**, *19*, 5735–5741.

(17) Eriksson, J.; Malmsten, M.; Tiberg, F.; Callisen, T. H.; Damhus, T.; Johansen, K. S. *J. Colloid Interface Sci.* **2005**, *284*, 99–106.

(18) Eriksson, J.; Malmsten, M.; Tiberg, F.; Callisen, T. H.; Damhus, T.; Johansen, K. S. *J. Colloid Interface Sci.* **2005**, *285*, 94–99.

(19) Penfold, J.; Thomas, R. *J. Phys.: Condens. Matter* **1990**, *2*, 1369–1412.

(20) Beldman, G.; Searle-Van Leeuwen, M. F.; Rombouts, F. M.; Voragen, G. J. *Eur. J. Biochem.* **1985**, *146*, 301–308.

(21) Rivera-Armenta, J. L.; Heinze, T.; Mendoza-Martinez, A. M. *Eur. Polym. J.* **2004**, *40*, 2803–2812.

(22) Kaya, A.; Du, X.; Liu, Z.; Lu, J. W.; Morris, J. R.; Glasser, W. G.; Heinze, T.; Esker, A. R. *Biomacromolecules* **2009**, *10*, 2451–2459.

(23) Kontturi, E.; Suchy, M.; Penttila, P.; Jean, B.; Pirkkalainen, K.; Torkkeli, M.; Serimaa, R. *Biomacromolecules* **2011**, *12*, 770–777.

(24) Kienzle, P. A.; Doucet, M.; McGillivray, D. J.; O'Donovan, K. V.; Berk, N. F.; Majkrzak, C. F. http://www.ncnr.nist.gov/reflpak. 2000−2006.

(25) Russell, T. *Mater. Sci. Rep.* **1990**, *5*, 171–271.

(26) Heinrich, F.; Ng, T.; Vanderah, D. J.; Shekhar, P.; Mihailescu, M.; Nanda, H.; Losche, M. *Langmuir* **2009**, *25*, 4219–4229.

(27) Hine, J.; Thomas, C. H. *J. Am. Chem. Soc.* **1953**, *75*, 739–740.

(28) Rodahl, M.; Hook, F.; Krozer, A.; Brzezinski, P.; Kasemo, B. *Rev. Sci. Instrum.* **1995**, *66*, 3924–3930.

(29) Mazeau, K.; Heux, L. *J. Phys. Chem. B* **2003**, *107*, 2394–2403.

(30) Weimer, P. J.; Lopez-Guisa, J. M.; French, A. D. *Appl. Environ. Microbiol.* **1990**, *56*, 2421–2429.

(31) Kontturi, E.; Lankinen, A. *J. Am. Chem. Soc.* **2010**, *132*, 3678–3679.

(32) Mark, H. F. In *Encyclopedia of Polymer Science and Technology - Plastics, Resins, Rubbers, Fibers*; Wiley: New York, 1982; Vol. 3.

(33) Crawshaw, J.; Vickers, M. E.; Briggs, N. P.; Heenan, R. K.; Cameron, R. E. *Polymer* **2000**, *41*, 1873–1881.

(34) Marcus, Y.; Ben-Naim, A. *J. Chem. Phys.* **1985**, *83*, 4744–4759.

(35) Graziano, G. *J. Phys. Chem. B* **2000**, *104*, 9249–9254.

(36) Battistuzzi, G.; Borsari, M.; Ranieri, A.; Sola, M. *JBIC, J. Biol. Inorg. Chem.* **2004**, *9*, 781–787.

(37) Hook, F.; Kasemo, B.; Nylander, T.; Fant, C.; Sott, K.; Elwing, H. *Anal. Chem.* **2001**, *73*, 5796–5804.

(38) Voinova, M. V.; Rodahl, M.; Jonson, M.; Kasemo, B. *Phys. Scr.* **1999**, *59*, 391–396.